Dynamic Jahn-Teller distortions and thermal conductivity in $La_{1-x}Sr_xMnO_3$ crystals

J.-S. Zhou and J. B. Goodenough
Texas Materials Institute, ETC 9.124, University of Texas at Austin, Austin, Texas 78712
(Received 10 April 2001; published 21 June 2001)

A systematic measurement of thermal conductivity $\kappa(T)$ below room temperature has been carried out on a series of single-crystal samples of $La_{1-x}Sr_xMnO_3$ that were chosen to probe changes on crossing several crystallographic phases and electronic phase transitions. The data show that the lattice component of $\kappa(T)$ is strongly suppressed at the transition from localized to itinerant electronic behavior and in localized-electron phases with orbital fluctuations.

DOI: 10.1103/PhysRevB.64.024421 PACS number(s): 75.30.Et, 66.70.+f, 71.70.Ej

How heat transfers in the manganese-oxide perovskites provides information on the complex interplay between orbital, charge, and spin ordering, dynamic phase segregation, and charge transfer in these materials. Two previous studies[1,2] have reported a small, glasslike thermal conductivity $\kappa(T)$ in polycrystalline samples of $LaMnO_{3+\delta}$ and in single-crystal $LaMnO_3$ doped with Ca, Sr, or Pb. Cohn *et al.*[1] ascribed the suppression of $\kappa(T)$ in their ceramic sample $LaMnO_{3+\delta}$ to static local orbital ordering; Visser *et al.*[2] invoked local anharmonic lattice distortions to interpret a positive $d\kappa/dT$ above a ferromagnetic Curie temperature T_c. These earlier studies were unaware of several unusual phase transitions that have been revealed by transport and structural studies.[3–7] We report here measurements of $\kappa(T)$ below 300 K made on oxygen-stoichiometric single crystals of $La_{1-x}Sr_xMnO_3$ with x chosen to cover the transitions from localized-electron behavior with a cooperative Jahn-Teller distortion to itinerant σ-bonding $3d$ electrons through a crossover region with orbital and bond-length fluctuations. It is at this crossover that the colossal magnetoresistance (CMR) reaches its maximum.[8] Our data show unambiguously a close relationship between the orbital degrees of freedom and/or bond-length fluctuations at the Mn atoms and the remarkable suppression of the phonon contribution to $\kappa(T)$.

The transition on the MnO_3 array from the parent antiferromagnetic insulator to a ferromagnetic metallic phase having a mixed Mn(IV)/Mn(III) valence is complex; it can be traversed by controlling the nominal Mn(IV) concentration x and the geometric tolerance factor t by substitutions for La of an alkaline earth A and/or a smaller lanthanide ion Ln in $(La_{1-y}Ln_y)_{1-x}A_xMnO_3$. A sharp transition from a canted-spin antiferromagnetic phase to a spin-glass phase or a ferromagnetic phase occurs at a critical tolerance factor t_c for a given x or, at a critical x_c for a given y. In both cases, the ferromagnetic Curie temperature T_c increases dramatically with t or x over a small Δx or Δt on entering the ferromagnetic phase.[3,8] The system $La_{1-x}Sr_xMnO_3$ reveals most clearly the complexity of the transition from antiferromagnetic insulator to ferromagnetic metal. The richness of the phase diagram of Fig. 1 is due to the σ-bonding electrons of e-orbital parentage. With the exception of the transition at T_{LO}, this phase diagram has been established by neutron diffraction[7] as well as by magnetic studies and by measurement of transport properties of single crystals as a function of temperature and pressure.[3–6] Four crystallographic and three thermodynamically distinguishable ferromagnetic phases have been found in the narrow compositional range $0.11 < x < 0.17$. Over this range, the σ-bonding electrons transform from localized to itinerant character. Such a transition is commonly first order, which gives rise in perovskites to a double-well potential for the two equilibrium metal-oxygen bond lengths. The double-well potential produces bond-length fluctuations that appear to be responsible for the CMR phenomenon.[9]

Where the σ-bonding e electron is localized, it occupies a state that is orbitally twofold-degenerate in a cubic site, and a distortion of the site orders the electron into one of the orbitals because of a strong coupling of the electrons to the oxygen displacements. Cooperative distortions reduce the elastic energy associated with an individual distortion; the cooperativity may be long-range and static as occurs in $LaMnO_3$ or short-range and dynamic; of interest here is the influence of dynamic, short-range orbital ordering on the thermal conductivity.

In the O′ phases of Fig. 1, the e electrons are ordered into orbitals oriented in the (001) planes. At T^*, the orbital or-

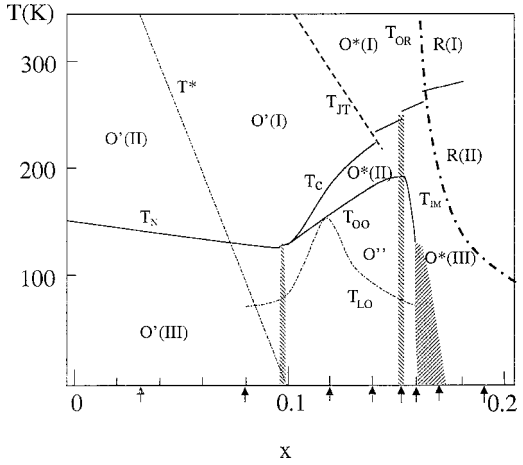

FIG. 1. Schematic phase diagram for $La_{1-x}Sr_xMnO_3$. O′(I): *P,I*; O′(II): *P,I*; O′(III): AF, *I*; O*(I): *P,I*; O*(II): SG, *C*; O*(III): *F,M*; O″:F,I; *R*(I): *P,C;R*(II): *F,M*. O′: orthorhombic $c/\sqrt{2} < a,b$; O*: orthorhombic $c/\sqrt{2} \approx a,b$; *R*: rhombohedral; O″: orthorhombic $c/\sqrt{2} \approx a,b$; *P*: paramagnetic; *F*: ferromagnetic; AF: antiferromagnetic; SG: spin glass; *I*: insulator; *C*: conductive; *M*: metallic.

dering changes from the static configuration of $LaMnO_3$ to two-dimensional (2D) fluctuations within the (001) planes; T_{JT} marks the onset of 3D orbital disorder. The rhombohedral phases contain itinerant electrons in σ^* bands; this symmetry does not lift the *e*-orbital degeneracy. The change from the O*(II) to the O* (III) phase at $x \approx 0.15$ is first order as also is the O″ to O* (III) transition at T_{IM}; these transitions mark a change from strong to weak electron-lattice coupling. The transition from the O*(II) to the O″ phase at T_{OO} is second-order except at the composition $x \approx 0.125$.

Single-crystal samples have been grown by the floating-zone method with IR-heating image furnaces at UT Austin and the University of Tokyo.[3] The samples made in UT-Austin are comparable with those made in the University of Tokyo where composition analysis has been carried out. A large thermoelectric power indicates that the parent compound $LaMnO_3$ had a Mn(IV) fraction less than 0.001. The thermal conductivity $\kappa(T)$ was measured with a steady-state method, and the system was calibrated with two known materials.

Heat is transferred primarily by electrons and phonons in crystalline materials. A general expression for the thermal conductivity is $\kappa = NC_p \upsilon l$, where N is the number of thermal carriers, C_p is the specific heat, υ is the drift velocity of the heat carriers, and l is their mean free path. At higher temperature, both electrons and phonons have an $l - 1/T$ that decreases with increasing temperature. At lower temperatures, l is limited by the crystal or grain size.[10] At higher temperatures, C_p becomes independent of temperature for phonons. In broadband metals, the electronic conductivity gives a good measure of $\kappa_{el}(T)$ at $T \geqslant \theta_D$ from the Wiedemann-Franz (WF) law. For metals at $T < \theta_D$ and narrow-band conductors, the WF law can still provide an upper bound of $\kappa_{el}(T)$.[10] Amorphous and glass insulators, on the other hand, have a small κ[1–5 W/(mK)] with a $d\kappa/dT > 0$ extending over a broad temperature range.[10]

Whereas Cohn *et al.*[1] reported a surprisingly small $\kappa(T)$ for their $LaMnO_3$ sample, our measurement on oxygen-stoichiometric single-crystal and Ar-annealed polycrystalline $LaMnO_3$ both showed a large, well-defined phonon contribution to $\kappa(T)$; see Fig. 2. The difference in the two curves at low temperatures reflects the grain-size limitation of *l*. An abrupt change of $\kappa(T)$, and more clearly of $\kappa^{-1}(T)$, at T_N in the crystal of $LaMnO_3$ reflects an additional contribution from spin waves in the magnetic phase and the enhancement is accounted for in terms of the data of neutron inelastic scattering. A ceramic $LaMnO_{3.07}$ sample was found to have a greatly reduced $\kappa(T)$ and a $d\kappa/dT > 0$ like that reported by Cohn *et al.*[1] in their ceramic ''$LaMnO_3$'' sample. The results show unambiguously that $\kappa(T)$ is dominated by phonons where the orbital ordering is static, but it is suppressed to glass-like behavior by the introduction of holes into the MnO_3 array. $\kappa_{el}(T)$ is negligible in this case and the introduction of a few cation vacancies in the oxidized samples should not reduce $\kappa_{latt}(T)$ dramatically. Therefore, the glass-like $\kappa(T)$ found in $LaMnO_{3+\delta}$ must be related to bond-length fluctuations associated with the formation of polarons or with the transition from static orbital ordering to 2D or 3D

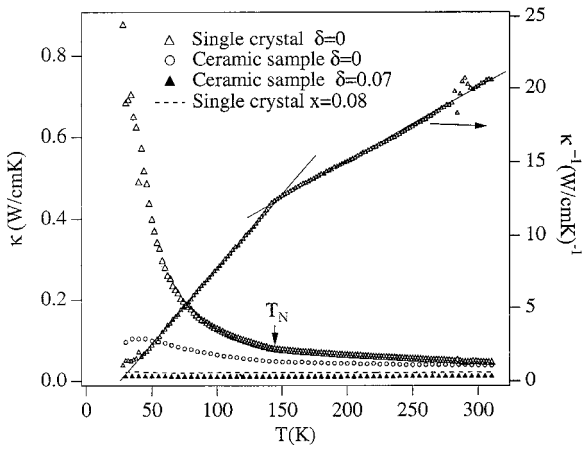

FIG. 2. Temperature dependence of thermal conductivity κ and κ^{-1} for single-crystal $LaMnO_{3.00}$, $La_{0.97}Sr_{0.03}MnO_3$, and ceramic samples $LaMnO_{3+\delta}$ ($\delta = 0,\ 0.07$). The lines in the curve κ^{-1} versus T are linear fitting.

orbital disorder. The correlation of bond-length fluctuations with a suppression of $\kappa_{latt}(T)$ is further demonstrated in the $La_{1-x}Sr_xMnO_3$ system.

As marked by arrows in Fig. 1, hole concentrations x in $La_{1-x}Sr_xMnO_3$ were chosen to cover the area in the phase diagram where several phase transitions occur. Given the transport and structural data used to obtain Fig. 1, it becomes possible for us to understand the complicated $\kappa(T)$ data shown in Fig. 3. No anomaly of the resistivity $\rho(T)$ has been found in the $x = 0.08$ sample; its $\kappa(T)$, plotted in Fig. 2, shows almost the same temperature dependence as that of $LaMnO_{3.07}$ except at very low temperatures where the polaron motion is frozen out. The $\rho(T)$ data are plotted together with $\kappa(T)$ in Fig. 3 for each of the compositions to indicate the electronic transitions that occur at the structural transitions. The $\kappa_{el}(T)$ calculated from the WF law for the $x = 0.12$ and 0.14 samples is smaller than $\kappa(T)$ by a few orders of magnitude; the $\kappa(T)$ measured should be treated as the contribution from the lattice. On lowering the temperature from room temperature, both the $x = 0.12$ and the 0.14 crystals undergo three transitions at T_{JT}, T_c, and T_{OO} as marked for each sample. A $d\kappa_{latt}(T)/dT > 0$ has been found in both O′(I) and O* phases; the magnitude of $\kappa_{latt}(T)$ falls close to the level of a glass insulator.[10] However, a jump of $\kappa_{latt}(T)$ at T_{JT} indicates that the O′(I) phase with 2D orbital disorder is more thermally conductive than the O*(I) phase with 3D orbital disorder. The $\kappa_{latt}(T)$ falls as the O* phase is restored below T_c in the ferromagnetic O*(II) conductive phase; any spin-wave enhancement of $\kappa(T)$ below T_c is dominated by the suppression of $\kappa(T)$ at the transition from the O′(I) phase to the O*(II) phase. Because T_{JT} is so close to T_c in the $x = 0.14$ crystal, the jump of $\kappa(T)$ at T_{JT} and the drop at T_c are nearly combined. For the crystal $x = 0.12$, the transition at T_{OO} was found to be first-order from the $\rho(T)$ and neutron-diffraction data.[4,11] A big jump in κ on cooling through T_{OO} followed by a $\kappa(T) \sim T^{-1.5}$ demonstrates restoration of κ_{latt} in the O″ phase of this sample. Although no charge ordering was found in the insulator phase below T_{OO},[12] a significant restoration of the κ_{latt} occurs as a result

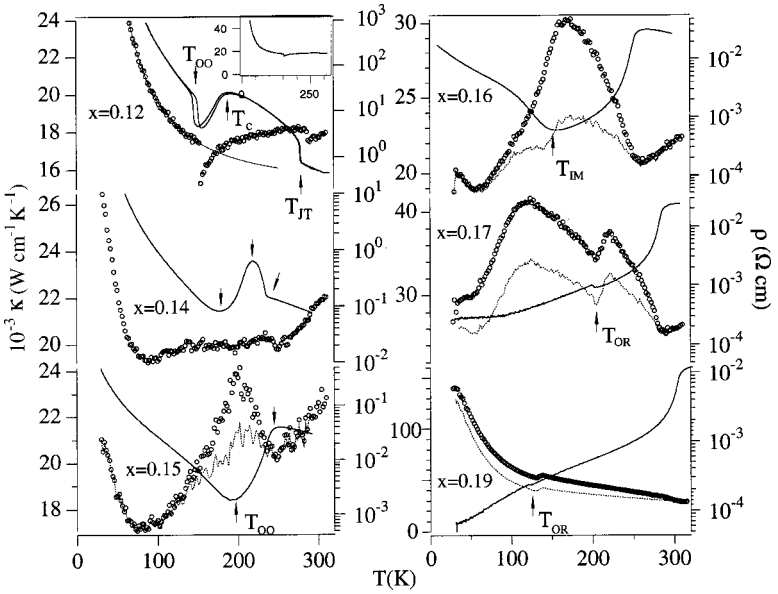

FIG. 3. Temperature dependence of thermal conductivity κ and resistivity ρ for selected single-crystal samples of the system $La_{1-x}Sr_xMnO_3$. The symbol circle for the measured κ; dashed line for the $\kappa-\kappa_{el}$, solid line for the resistivity; the line with $\kappa(T)$ below T_{OO} is a fitting to the formula $T^{-1.5}$. The inset is a full-range plot of the $\kappa(T)$ for the $x=0.12$ sample.

of orbital ordering. However, the $x=0.12$ sample is distinguishable below T_{OO} from its neighbors; the $\kappa_{latt}(T)$ for the compositions away from $x=1/8$ remain suppressed in the O″ phase above a temperature T_{LO}. This compositional singularity at $x=1/8$ in the phase diagram underscores the possibility of a charge commensuration like that found in the $(La_{1-y}Nd_y)_{2-y}Sr_xCuO_4$ system.[13]

In the crystals $x=0.15$, 0.16, 0.17, and 0.19, a lower $\rho(T)$ makes it necessary to subtract out the electronic contribution from the measured $\kappa(T)$ in Fig. 3. The resulting $\kappa_{latt}(T)$ is a lower bound for the lattice contribution. In the $x=0.16$ crystal, $\kappa_{latt}(T)$ is enhanced below T_c, which is remarkably different from its behavior in the $x=0.14$ crystal. We have detected a phase boundary below T_c in a narrow range $0.14<x\leqslant 0.15$; T_c shows a discontinuous jump at the boundary, and a transition from a vibronic state to an itinerant electronic state has been proposed.[5] The $\kappa(T)$ data shown in Fig. 3 support this argument since heat-carrying phonons would be released in an itinerant electron state where the electron-lattice coupling is reduced; the $x=0.15$ crystal is located at the boundary.

The resistivity of the O″ phase changes by over six orders within a narrow compositional range $0.1<x\leqslant 0.16$. Although the transport properties[4] suggest a phase boundary below T_{OO} near $x=0.15$, neutron-diffraction data[12] show a nearly identical structure over the entire range. With the exception of the $x=0.12$ crystal, $\kappa_{latt}(T)$ remains suppressed except at very low temperatures in the O″ phase. The axial ratio $c/a \leqslant\sqrt{2}$ in this phase allows 2D orbital disorder or fluctuations that may be correlated with the suppression of $\kappa_{latt}(T)$. This orbital disorder does not disrupt the ferromagnetism in this phase; neither does orbital order in the ferromagnetic $x=0.12$ sample. The low $\rho(T)$ and a $d\rho/dT>0$ of the $x=0.17$ crystal would seem to imply that T_{IM} is lowered to below 4 K. However, $\kappa_{latt}(T)$ decreases below about $T=120$ K in the same manner it does below T_{IM} in the $x=0.16$ sample. This reduction of $\kappa_{latt}(T)$ can be attributed to two phase fluctuations that have been identified at the boundary of the first-order transition from the O″ to the O*(III) phase.[6] The $x=0.19$ sample is fully metallic below room temperature, and a typical phonon contribution appears in $\kappa_{latt}(T)$. The large magnitude of κ_{latt}, its power-law temperature dependence, and its peaking at very low temperature all show the superior quality of the crystal; a comparable behavior has not been found in either the metallic ceramic sample $La_{0.7}Ca_{0.3}MnO_3$ (Ref. 1) or the metallic single-crystal sample $La_{0.4}Pb_{0.4}MnO_3$.[2] A drop in $\kappa(T)$ occurs at T_{OR} on cooling from the R(II) to the O*(III) phase. The $\rho(T)$ data show that this drop cannot be attributed to a change in $\kappa_{el}(T)$; it reflects a change in $\kappa_{latt}(T)$ due to a strong electron-lattice coupling in the O*(III) phase.

From the phase diagram in Fig. 1, the line of $T=50$ K cuts through insulator or polaron phases to a typical metallic phase. Except for the singularity near $x=1/8$, $\kappa_{latt}(50\,\mathrm{K})$ plotted in Fig. 4 is suppressed dramatically at the crossover from localized to itinerant electronic behavior. Accompany-

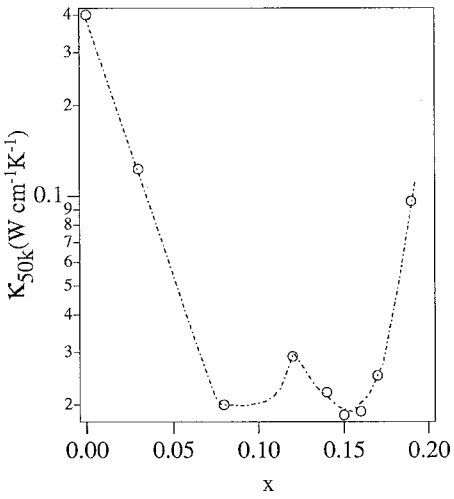

FIG. 4. Thermal conductivity at $T=50$ K as a function of x for $La_{1-x}Sr_xMnO_3$.

ing this crossover are transitions from a static cooperative Jahn-Teller distortion to orbital fluctuations and finally to the disappearance of localized orbitals. The difference in the $\kappa_{\text{latt}}(50\,\text{K})$ of the $x=0$ and $x=0.19$ samples might be attributable to *A*-site La/Sr disorder and a small change in the Debye temperature. However, the difference between $\kappa_{\text{latt}}(50\,\text{K})$ for the $x=0.19$ crystal and the crystals $x=0.08$, 0.14, 0.15, 0.16, 0.17 should be accounted for by bond-length fluctuations and electron-phonon interactions that are strong enough to suppress heat transfer through the phonons for the crystals $(0.1\leqslant x\leqslant 0.17)$. A similar plot has been observed at the metal-insulator transition in $BaCo_{1-x}Ni_xS_2$.[14] However, the minimum of κ_{latt}, in $La_{1-x}Sr_xMnO_3$ is broader than that in $BaCo_{1-x}Ni_xSi_2$, which might be caused by the orbital fluctuations in the former. From the jump of κ_{latt} at T_{OO} and T_{JT} in the $x=0.12$ sample, and at T_{OR} in the $x=0.17$ sample, we can clearly see the influence on thermal conductivity due to order-disorder orbital transitions. However, it is impossible to determine the effect numerically as the orbitals are not fully disordered in the O* phase at $T\geqslant T_{OO}$ and the restoration of orbital ordering in the O(I) phase appears to be only one-dimensional, orbital fluctuations being retained in the (001) planes.

On traversing the crossover from localized to itinerant electronic behavior, the electronic transfer time τ must experience a transition from $\tau>\omega_0^{-1}$ to $\tau<\omega_0^{-1}$, where ω_0^{-1} is the period of the cooperative oxygen vibrations to which the electrons are strongly coupled. At the crossover $\tau\approx\omega_0^{-1}$, the quasiparticle nature from both subspaces may be hybridized to form vibronic states. Neutron diffraction shows an enhancement of the Debye-Waller factor below T_c compared with that of the O′(I) phase in the $x=0.13$ sample.[7] The strong interaction between the electrons and the lattice vibrations may not destroy the phonon structure, but hybridization between electrons and phonons as found in $La_{0.8}Ca_{0.2}MnO_3$ by neutron diffraction[15] apparently suppresses the lattice component of the thermal conductivity.

In conclusion, both the insulator $LaMnO_3$ with a static cooperative Jahn-Teller distortion and the metallic phase in $La_{0.81}Sr_{0.19}MnO_3$ have shown a well-defined thermal conductivity from phonons. Suppression of the lattice component of the thermal conductivity has been observed in the narrow compositional range $0.1<x\leqslant 0.17$ where there is a crossover from localized to itinerant electronic behavior that is characterized by Mn-O bond-length fluctuations. This range appears to be broadened by the presence of Jahn-Teller orbital fluctuations. The conductive phase below T_c in the O*(II) phase of the $x=0.14$ crystal has a lower κ_{latt} than that in the metallic O*(III) phase of the $x=0.16$ sample. This observation supports the deduction from the transport properties that the O*(II) phase in the range $T_{OO}<T<T_c$ is vibronic.

We thank the NSF and both the TCSUH and the Robert A. Welch Foundation of Houston, TX, for financial support. We thank Professor A. Asamitsu and Professor Y. Yokura for providing some crystals of this work, and Professor P. B. Allen for enlightening us of the enhancement of κ for $LaMnO_3$ in terms of neutron-inelastic-scattering data.

[1] J. L. Cohn, J. J. Neumeier, C. P. Popoviciu, K. J. McClellan, and Th. Leventouri, Phys. Rev. B **56**, R8495 (1997).
[2] D. W. Visser, A. P. Ramirez, and M. A. Subramanian, Phys. Rev. Lett. **78**, 3947 (1997).
[3] A. Urushibasa, Y. Moritomo, T. Arima, A. Asamitsu, G. Kido, and Y. Tokura, Phys. Rev. B **51**, 14 103 (1995).
[4] J.-S. Zhou, J. B. Goodenough, A. Asamitsu, and Y. Tokura, Phys. Rev. Lett. **79**, 3234 (1997).
[5] J.-S. Zhou and J. B. Goodenough, Phys. Rev. B **62**, 3834 (2000).
[6] J.-S. Zhou, G. Liu, and J. B. Goodenough, Phys. Rev. B **63**, 172416 (2001).
[7] B. Dabrowski, X. Xiong, Z. Bukowski, R. Dybzinski, P. W. Klamut, J. E. Siewenie, O. Chmaissem, J. Shaffer, C. W. Kimball, J. D. Jorgensen, and S. Short, Phys. Rev. B **60**, 7006 (2000).
[8] H. Y. Hwang, S-W. Cheong, P. G. Radaelli, M. Marezio, and B. Batlogg, Phys. Rev. Lett. **75**, 914 (1995).
[9] J. B. Goodenough, Aust. J. Phys. **52**, 155 (1999).
[10] R. Berman, *Thermal Conductivity in Solids* (Oxford University Press, New York, 1996).
[11] Y. Yamada, O. Hino, S. Nohdo, R. Kanao, T. Inami, and S. Katano, Phys. Rev. Lett. **77**, 904 (1996).
[12] Y. Endoh, K. Hirota, S. Ishihara, S. Okamoto, Y. Murakami, A. Nishizawa, T. Fukuda, H. Kimura, H. Nojiri, K. Kaneko, and S. Maekawa, Phys. Rev. Lett. **82**, 4328 (1999).
[13] J. M. Tranquada, B. J. Sternlieb, J. D. Axe, Y. Nakamura, and S. Uchida, Nature (London) **365**, 561 (1995).
[14] J. Takeda, J. Sakurai, A. Nakamura, M. Kato, Y. Kobayashi, and M. Sato, J. Phys. Soc. Jpn. **68**, 1602 (1999).
[15] P. Dai, H. Y. Hwang, J. Zhang, J. A. Fernandez-Baca, S. W. Cheong, C. Kloc, Y. Tomioka, and Y. Tokura, Phys. Rev. B **61**, 9553 (2000).